

Article

Optimization for Offshore Prestressed Concrete–Steel Hybrid Wind Turbine Support Structure with Pile Foundation Using a Parallel Modified Particle Swarm Algorithm

Zeyu Li ¹ , Bin Xu ^{2,3,*}  and Guokai Yuan ⁴

¹ College of Civil Engineering, Hunan University, Changsha 410082, China; lizeyu@hnu.edu.cn

² College of Civil Engineering, Huaqiao University, Xiamen 361021, China

³ Key Laboratory for Intelligent Infrastructure and Monitoring of Fujian Province, Huaqiao University, Xiamen 361021, China

⁴ China Energy Engineering Group Guangdong Electric Power Design Institute Co., Ltd., Guangzhou 510663, China; yuanguokai@gedi.com.cn

* Correspondence: binxu@hqu.edu.cn

Abstract: The prestressed concrete–steel hybrid (PCSH) support structure, which replaces the lower part of the traditional support with a concrete segment, is a prospective support structure solution for ultrahigh wind turbines. Taking a 5.5 MW wind turbine support structure founded on a jacket substructure with pile foundation as an example, an optimized design of the corresponding PCSH support structure with pile foundation for offshore wind turbine is conducted considering the soil–structure interaction (SSI) and the effect of water pressure. The construction cost of the proposed structure is treated as the objective function and minimized with a parallel modified particle swarm optimization (PMPSO) algorithm where the physical dimensions of each part of the PCSH wind turbine support structure are treated as optimization variables. Eleven optimization constraints are considered under both the serviceability limit state (SLS) and the ultimate limit state (ULS) according to relevant specifications and industry standards. A penalty function strategy is introduced to make sure that these constraints are fulfilled. The mechanical behavior and the cost of the optimal PCSH support structure with pile foundation are analyzed and are compared with those of the original design with a traditional steel tube tower founded on a jacket substructure. The results show that the cost and leveled cost of energy (LCOE), a comprehensive evaluation, of the optimized PCSH support decrease obviously with the PMPSO algorithm, which can provide advanced mechanic behavior including natural frequency, top deformation, and anti-overturning capacity. Compared with the PSO algorithm, the PMPSO algorithm has better performance in the procedure of PCSH support for offshore wind turbine optimization.

Keywords: prestressed concrete–steel hybrid (PCSH) wind turbine support; optimal design; parallel modified particle swarm optimization (PMPSO) algorithm; pile foundation



Citation: Li, Z.; Xu, B.; Yuan, G. Optimization for Offshore Prestressed Concrete–Steel Hybrid Wind Turbine Support Structure with Pile Foundation Using a Parallel Modified Particle Swarm Algorithm. *J. Mar. Sci. Eng.* **2024**, *12*, 826. <https://doi.org/10.3390/jmse12050826>

Academic Editor: Muk Chen Ong

Received: 16 April 2024

Revised: 12 May 2024

Accepted: 14 May 2024

Published: 15 May 2024



Copyright: © 2024 by the authors. Licensee MDPI, Basel, Switzerland. This article is an open access article distributed under the terms and conditions of the Creative Commons Attribution (CC BY) license (<https://creativecommons.org/licenses/by/4.0/>).

1. Introduction

For the past few years, the development of offshore wind power in China has become increasingly attractive because of abundant, steady and strong wind resources and available spaces for offshore wind turbine installation in the southeast coast to meet the strong power needs in most electricity-poor developed cities. Traditional steel towers have been widely employed in offshore wind turbine support structures with various substructures, such as monopile, jacket, and gravity base foundations [1,2]. Wang [3] presented a transformed linear Gaussian model for generating equivalent “nonlinear” irregular waves to assess the mechanical responses of an offshore jacket wind turbine support. Based on elastic and plastic analyses of monopile foundation, Campione [4] proposed a simplified approach to calculate the soil–structure interaction (SSI) of offshore wind tower founded

on a monopile member. Aidibi et al. [5] investigated the stress concentration of the joints by using analytical calculations and numerical solutions. The results show that the stress concentration factors from the standards are more conservative than those from the finite element method. Unfortunately, the most widely used support structures for offshore wind turbines may not be economical enough for the construction of offshore wind turbines with huge capacity in deep seas [6].

The concrete structure is an attractive alternative for lower production costs, better durability, and lower corrosion protection and maintenance costs, especially in salty atmospheres and harsh environments. Tu et al. [7] investigated the nonlinear dynamic response of the concrete-based structure with infill aggregates for offshore wind turbines. The results show that the dynamic response of the gravity base foundation under combined wind and wave loads exhibits similar but less smooth curves to that under the wind loads only. Vølund [8] compared the costs of utilizing concrete foundations against steel monopile foundations for offshore wind turbines and discovered that the concrete foundation can greatly reduce the investment of wind turbine support structures. Ma and Yang [9] proposed and investigated a novel hybrid monopile foundation for an offshore wind turbine tower by replacing the conventional substructure with a steel–concrete hybrid structure. Lian et al. [10] and Zhai et al. [11] numerically and experimentally studied a suction bucket foundation with a prestressed concrete (PC) substructure for a 2.5 MW offshore wind turbine and verified its feasibility, respectively.

Prestressed concrete–steel hybrid (PCSH) wind turbine towers have been an attractive alternative for onshore wind turbine tower design. Chen et al. [12] investigated the seismic responses of the PCSH wind turbine tower and indicated that time history analyses should be a necessary supplement for its seismic design. Huang et al. [13] conducted a sensitivity analysis to study the relationship between the natural frequency and the dimensions of PCSH wind turbine towers and optimized a 160 m PCSH wind turbine tower. Li et al. [14] proposed a two-scale model to explore the global and local mechanical behavior of PCSH wind turbine tower.

The cost of maintaining, installing, and manufacturing offshore wind turbine support structures occupies at least 30–50% of the overall capital cost [15]. Several attempts have been made to find a cost-efficient support structure to make offshore wind energy compete with other traditional energy resources [16,17]. Optimization of all wind turbine support structures is critical for the realization of potential cost benefits and safety requirements. Kaveh and Sabeti [18] optimized jacket support structures for offshore wind turbines utilizing the colliding bodies optimization algorithm and approximately halved the weight of the structure. Treating the frequency as the optimal objective, Natarajan et al. [19] optimized the jacket offshore support structures for 10 MW wind turbines to alleviate the fatigue damage. Integrating kriging-based heuristic optimization, Mathern et al. [20] carried out an approach to optimize the wind turbine foundation of a Swedish wind farm and concluded that the proposed method can provide good-quality designs with an initial sample size of only 20 designs.

In this paper, an offshore PCSH wind turbine support structure with a foundation composed of four steel piles is first proposed. The lower part of the traditional steel tube support tower and the substructure of a jacket-type offshore wind turbine platforms are replaced with PC tube. Then, taking a four-pile jacket-type 5.5 MW offshore wind turbine support structure with a hub elevation of 102.3 m as an example, the optimal design of the proposed alternative PCSH support structure with a four-pile foundation is investigated using a parallel modified particle swarm optimization (PMPSO) algorithm, where environmental influences, including the wind and wave loads, the seismic effect and the SSI are considered. The objective is to minimize the construction cost, and the optimization results for the PCSH support structure are compared with those of the original design. The results show that the optimal PCSH support structure can fulfill the design requirements but with a lower construction cost and comprehensive investment when compared with the original design. In addition, the optimal design results show that the

steel tube of the optimized PCSH structure is suggested to occupy about 25.8% of the overall height of the PCSH support structure. Finally, the mechanical behavior of the optimal PCSH support structure with pile foundation is analyzed and compared with that of the traditional steel support structure.

2. Concept Description

In this paper, referring to the overall PC offshore wind turbine substructure proposed by Lian et al. [10], a PC segment is adopted to replace the lower part of the traditional full-height tapered steel tube tower and the substructure of the offshore wind turbine support structure to decrease the construction cost of the offshore wind turbine. The proposed offshore PCSH support structure with a four-pile foundation consists of the PC substructure and PCSH tower, as illustrated in Figure 1.

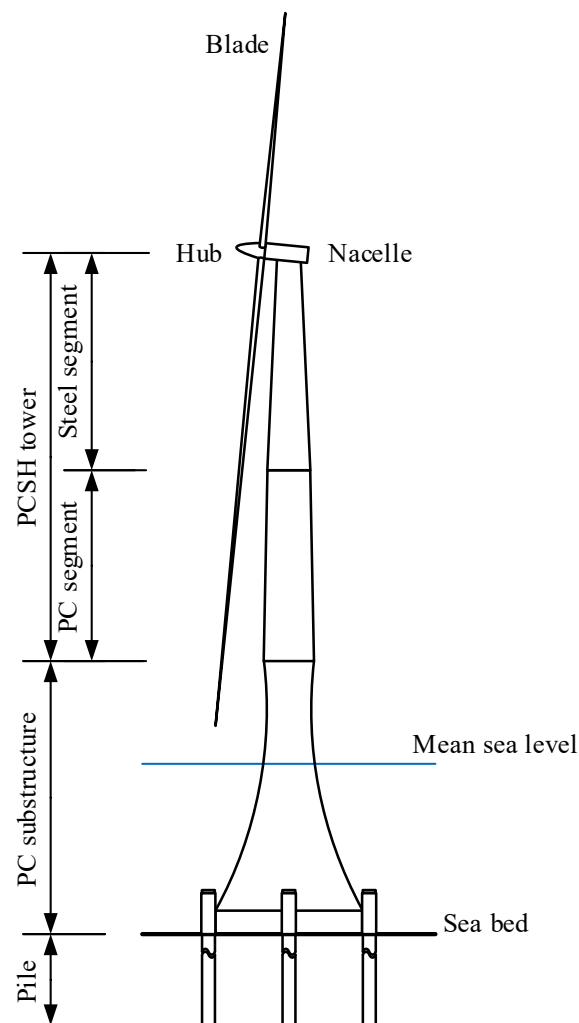


Figure 1. Description of offshore PCSH support.

The lower part of the tower and the substructure are made of PC and the tower's upper segment is a conventional tapered steel tube tower. Like the PC foundation for offshore wind turbines [10], the offshore PCSH support can be fabricated onshore and towed to the designated construction site, and then submerged [21]. Pile foundations are employed to reduce the weight of the structures when the wind turbine supports are built in soft clay [22]. Compared with a traditional pure steel tube support structure, the PCSH structure reasonably results in a cheaper construction investment, lower center of gravity, better integrity, higher flexural stiffness, lower cost for corrosion protection, and less maintenance, especially in harsh environments. Therefore, the PCSH structure is a promising alternative

for the offshore wind turbine support structures. The optimization of the proposed PCSH support structure with a pile foundation is critical and to be addressed in this study.

3. Numerical Model and Loading Combination

3.1. Mathematical Model

In the mathematical model of the offshore PCSH wind turbine support structure, the stress distribution near the flange and the door opening are not taken into account. The model is based on the linear material and small deformation assumption, and only the fore-aft direction is considered [23].

3.1.1. Five Lumped Mass Model for the Offshore PCSH Wind Turbine Support Structure

In this study, the offshore PCSH wind turbine support structure with pile foundation is modeled as a five lumped mass model as illustrated in Figure 2 [24]. The m_5 in Figure 2 is the heaviest due to the existence of Rotor-Nacelle Assembly (RNA) and blades, and the rest of the lumped mass can be calculated based on the distributed mass of the structure.

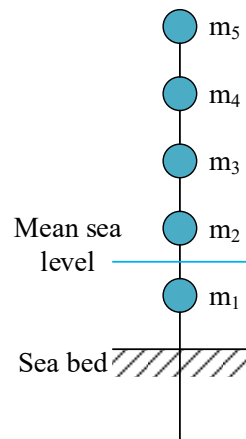


Figure 2. Simplified tower model.

According to the five lumped mass model, the natural frequencies of the PCSH support without considering the effect of water and pile–soil interaction can be obtained by the following equation:

$$\left| \delta M - \frac{1}{\omega^2} \right| = 0 \tag{1}$$

where δ and M are the flexibility and mass matrix of the PCSH support structure, respectively, and ω is the circular frequency.

3.1.2. Added Mass Method Considering the Dynamic Water Pressure

The added mass method is adopted to consider the influence of dynamic water pressure on the dynamic characteristics of the PC substructures [25]. For a circular section of the PCSH structure, the additional mass per unit length of a circular substructure Δm_{cir} can be calculated by the following equations:

$$\Delta m_{cir} = \rho_{con} \left(\pi D^2 / 4 \right) p_{cir}(d, D) \tag{2}$$

$$p_{cir}(d, D) = [0.0133 \ln(d) - 0.0112] \ln(D) + 0.0002d + 0.4 \tag{3}$$

where ρ_{con} is the density of concrete, D is the diameter of the circular section of the structure, and d is the depth of the water.

The equivalent mass per unit length of the model \tilde{m} can be calculated by the following formula:

$$\tilde{m} = m + \Delta m_{cir} \tag{4}$$

where m is the mass per unit length of the circular section of the structure.

3.1.3. Interaction between Piles and Soil

The offshore PCSH wind turbine support structure with pile foundation proposed in this study is for soft soil conditions and it is critical to consider the SSI between the pile foundation and the soil.

In this section, the piles are considered semi-infinite piles since $\beta l = 7.35 > \pi$, in which β is the eigenvalues of the piles and l is the length of the piles. The ground is treated as a single-layer ground due to the similarity of the soil in the depth range of $1/\beta$ [26]. The group pile effect is not considered because the distance between piles is 5.5 times larger than the pile diameter. Therefore, the piles of the PCSH structure are considered as a beam and the soil is assumed to be elastic [27].

As shown in Figure 3, the deflection of the structure $y_F(x)$ with a hypothetical horizontal force F acting at the top of the tower can be evaluated by the following formula:

$$y_F(x) = y_{F1}(x) + y_{F2}(x) \tag{5}$$

in which the structural deflection caused by the deformation of the bottom of the substructure $y_{F1}(x) = \theta_0 x + y_0$, $y_{F2}(x)$ is the deflection without considering the influence of interaction between the pile and the soil, and θ_0 and y_0 are the rotation and deflection at the bottom of the substructure, respectively.

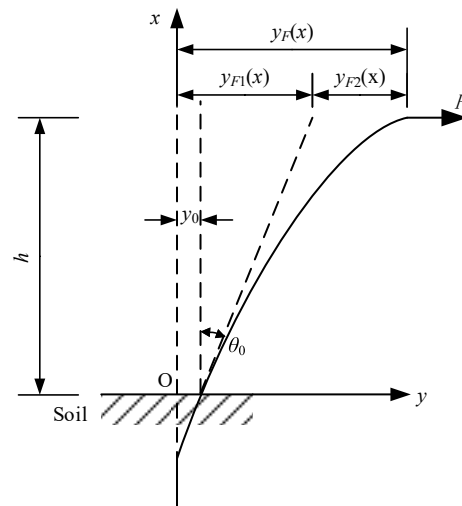


Figure 3. Deformation of structure with hypothetical horizontal force F acting at the top of the tower.

The horizontal deflection of the pile foundation can be estimated by [28]:

$$y = \frac{F}{2E_z I_z \beta^3} e^{-\beta z_p} [(1 + \beta h) \cos \beta z_p - \beta \sin \beta z_p] \tag{6}$$

where E_z and I_z are the elastic modulus and inertial moment of the piles, respectively, h is the height of the force point, and z_p is the depth of the pile.

Therefore,

$$\theta_0 = y'(z_p = 0) = \frac{F}{2E_z I_z \beta^2} (1 + 2\beta h) \tag{7}$$

$$y_0 = y(z_p = 0) = \frac{F}{2E_z I_z \beta^3} (1 + \beta h) \tag{8}$$

Substitute Equations (7) and (8) into Equation (5),

$$y_F(h) = \frac{F}{2E_z I_z \beta^3} (1 + \beta h) + \left[\frac{F}{2E_z I_z \beta^2} (1 + \beta h) + \frac{Fh}{2E_z I_z \beta} \right] h + y_{F2}(h) \tag{9}$$

Therefore, the flexibility matrix δ in Equation (1) can be expressed as $\tilde{\delta}$:

$$\tilde{\delta}_{ij} = \frac{1}{2E_z I_z \beta^3} (1 + \beta h_i) + \left[\frac{1}{2E_z I_z \beta^2} (1 + \beta h_i) + \frac{h_i}{2E_z I_z \beta} \right] h_{ij} + \delta_{ij} \quad (10)$$

where h_i is the height of the lumped mass i .

According to Equations (4) and (10), Equation (1) for the PCSH support should be reformulated as the following equation:

$$\left| \tilde{\delta} \tilde{M} - \frac{1}{\omega^2} \right| = 0 \quad (11)$$

where $\tilde{\delta}$ and \tilde{M} are the equivalent flexibility and equivalent mass matrix of the PCSH support structure, respectively.

3.2. Wave and Current Loads

The wave and current loads should be considered in the structural analysis and design of the PCSH structure as a type of offshore structure. The wavelength of the wave is generally greater than 130 m under extreme working conditions, which is larger than five times the diameter of the substructure. The wave loads can be predicted by Morison's equation [29].

$$df_H = \frac{1}{2} \rho_w C_D D |u| u dz + \rho_w C_M \frac{\pi D^2}{4} \frac{du}{dt} dz \quad (12)$$

where ρ_w is the density of seawater, C_D is the drag coefficient, C_M is the inertia coefficient, the velocity of the water $u = u_w + u_c$, u_w is the velocity of wave, and u_c is the velocity of current.

In this study, Stokes' second-order wave theory is adopted to simulate the wave profile based on the suggestion given by the US Navy's Coastal Engineering Research Centre [30,31]:

$$\begin{cases} \eta = \frac{H_w}{2} \cos \theta + \frac{\pi H_w^2}{4L} \left(1 + \frac{3}{2 \sinh^2(kd)} \right) \text{cth}(kd) \cos 2\theta \\ \Phi = \frac{H_w L}{2T} \frac{\cosh[k(z+d)]}{\sinh(kd)} \sin \theta + \frac{3\pi H_w^2}{16T} \frac{\cosh[2k(z+d)]}{\sinh^4(kd)} \sin 2\theta \end{cases} \quad (13)$$

where η is the surface wave profile, Φ is the velocity potential function, H_w is the wave height, θ is the phase of the wave, L is the wavelength, and k is the wave number.

3.3. Aerodynamic Load

The lateral wind loads caused by the wind turbine under normal operational and extreme-load cases are considered. The aerodynamic load under normal operational and extreme-load cases can be determined by [32]:

$$F_n = C_c C_p \rho V_n^2 \pi R^2 \quad (14)$$

$$F_e = 0.5 C_t \rho V_e^2 A \quad (15)$$

$$\rho = 0.00125 e^{-0.0001 z_e^3} \quad (16)$$

where F_n is the wind load under normal operational case, C_c is the aerodynamic load correction factor, C_p is the wind energy utilization coefficient, ρ is the air density, V_n is the wind speed under normal operational case, R is the impeller radius, F_e is the wind load under the extreme-load case, C_t is the drag coefficient, V_e is the 50-year extreme 3s gust extreme wind speed, A is the projected area of the blade, and z_e is the elevation of the wind turbine.

The moment including the pitching moment M_P and deflecting torque T can be calculated by the following equations [32]:

$$M_P = \frac{4}{27} \frac{\rho}{B} \pi R^3 (V_1^2 - V_2^2) \tag{17}$$

$$T = 0.23 \rho V_c^2 \pi R^2 e_w \tag{18}$$

where B is the number of blades, e_w is the vertical distance between the wheel center and the tower center, and V_1 and V_2 are the wind speeds at 2/3 of the impeller radius above and below the hub center, respectively.

The wind load acting upon the tower can be determined by following equations [33]:

$$F_i = \omega_k A_i \tag{19}$$

$$\omega_k = \beta_z \mu_s \mu_z \omega_0 \tag{20}$$

where F_i is the wind load on the tower section i , A_i is the wind area, ω_0 is the basic wind pressure, β_z is the wind vibration coefficient, and μ_s and μ_z are the wind load shape coefficient and wind pressure height coefficient, respectively, which can be determined by GB 50009-2012 [33].

3.4. Earthquake Effect

The earthquake effect has a significant influence on the structural safety of the offshore PCSH wind turbine support. Severe seismic occurrences are rare and it is reasonable to separately consider earthquake loads from other loads for offshore structures [34]. In this paper, the seismic loads are treated as static loads determined by the mode-superposition response spectrum method [35].

3.5. Permanent Load

The permanent loads, including the vertical force and moment, are caused by the weight of the wind power generation system, such as the substructure, the tower, the RNA and the blades, and can be obtained by the density and dimension of each part of the system.

3.6. Load Combination

Referring to relevant studies [9,33,35,36], two sets of load combinations, including ultimate limit state (ULS) and serviceability limit state (SLS), are adopted to assess the feasibility of the offshore PCSH support structure and to optimize the design of the proposed structure. In the SLS with a normal operational case and an extreme-load case, the effect of wave and current loads with a 50-year return period, and the effect of an earthquake are considered, a load factor of 1.0 for all load categories is used. In the ULS, a load factor of 1.0, 1.35, 1.35 and 1.4 is employed for permanent, seismic, wave and wind actions, respectively.

4. Parallel Modified Particle Swarm Optimization (PMPSO) Approach

4.1. Independent Optimization Variables

The definition and ranges of independent variables for the optimization of the proposed offshore PCSH support structure with a pile foundation are presented in Figure 4 and Table 1. In the design of the offshore wind turbine tower, wave loading is one of the most important factors that threaten the safety of offshore infrastructures. According to Equation (12), a reduction in the diameter of the substructure can effectively reduce the wave load acting on the substructure. As shown in Figure 4c, a second-order Bézier curve is adopted to describe the dimension of the substructure. The Bézier curve is obtained by taking the top and bottom outer vertices of the normal section of the substructure as the starting and ending points of the curve, respectively, and selecting a third point that is not co-linear with the two points. Meanwhile, since Morison’s equation is only applicable to

thin piles where the ratio of the pile diameter to the wave’s wavelength is less than 0.2, it is necessary to constrain the maximum radius $D_{z_{tm}}$ of the substructure.

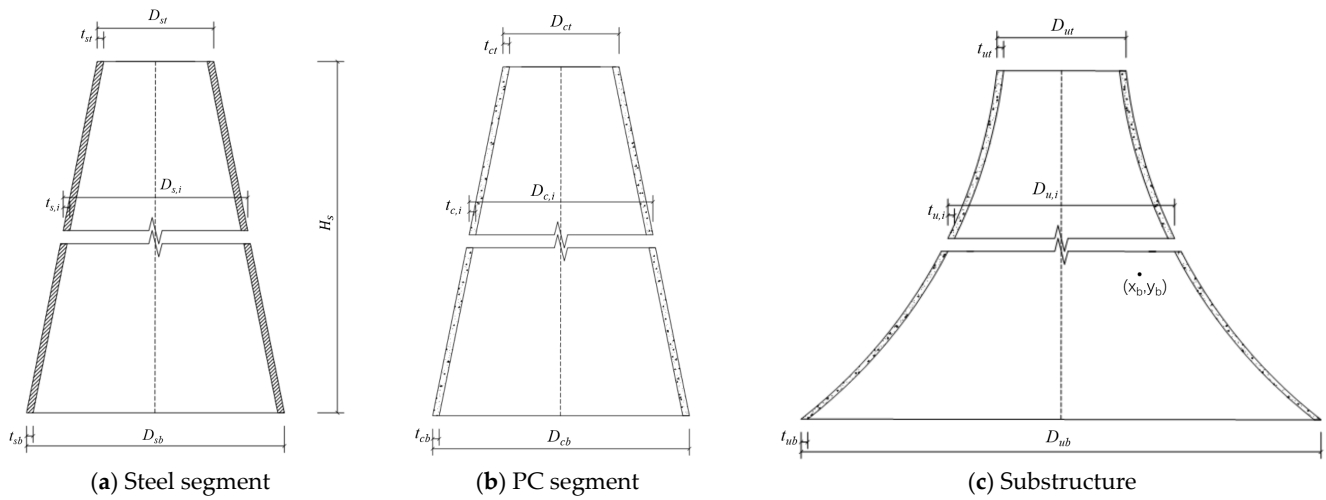


Figure 4. Design parameters of the offshore PCSH support structure.

Table 1. Variables and their ranges.

Variable	Range
H_s (mm)	2000–100,000
Area of prestressed reinforcement (mm^2)	20,000–100,000
t_{st} (mm)	10–50
t_{sb} (mm)	t_{st} -50
D_{st} (mm)	4050
D_{sb} (mm)	D_{st} -15,000
t_{ct} (mm)	180–800
t_{cb} (mm)	t_{ct} -800
D_{cb} (mm)	D_{sb} -35,000
t_{zt} (mm)	t_{cb} -800
t_{zb} (mm)	t_{zt} -800
D_{zb} (mm)	D_{zt} -35,000
Horizontal ordinate of the third point of the Bézier curve x_b (mm)	-25,000–0
Longitudinal ordinate of the third point of the Bézier curve y_b (mm)	D_{cb} - D_{zb}
Length of the piles (m)	70–100

4.2. Parallel Modified Particle Swarm Optimization (PMPSO) Algorithm

The particle swarm optimization (PSO) algorithm is an effective and widely used approach in structural optimal design. The structural optimization problem of PCSH support structure can be shown as follows:

$$\begin{cases} Z_{target} = \min f(\mathbf{x}) = \min f((x_1, x_2, \dots, x_n)^T) \\ h_c(\mathbf{x}) = [h_{c1}(\mathbf{x}), h_{c2}(\mathbf{x}), \dots, h_{cn}(\mathbf{x})]^T \leq 0 \end{cases} \quad (21)$$

where \mathbf{x} is the vector in n dimensions that stand for the particle, Z_{target} is the optimization target, $h_c(\mathbf{x})$ is the vector of constraint functions to present the safety of the structure, and $f(\mathbf{x})$ is a function to estimate the construction cost of the support, which can be calculated by the following formula:

$$f(\mathbf{x}) = V_{con}(\mathbf{x})p_{con}(\mathbf{x}) + V_{bar}(\mathbf{x})p_{bar}(\mathbf{x}) + V_{pre}(\mathbf{x})p_{pre}(\mathbf{x}) + V_{steel}(\mathbf{x})p_{steel}(\mathbf{x}) + V_{pile}(\mathbf{x})p_{pile}(\mathbf{x}) \quad (22)$$

where $V_{con}(\mathbf{x})$, $V_{bar}(\mathbf{x})$, $V_{pre}(\mathbf{x})$, $V_{steel}(\mathbf{x})$, $V_{pile}(\mathbf{x})$ are the volume of concrete, steel bar, prestressed tendon, steel tower and pile, respectively; and $p_{con}(\mathbf{x})$, $p_{bar}(\mathbf{x})$, $p_{pre}(\mathbf{x})$, $p_{steel}(\mathbf{x})$,

$p_{pile}(x)$ are the comprehensive unit price of concrete, steel bar, prestressed tendon, steel tower and pile, respectively.

Penalty function is adopted to transfer the constrained optimization problem to the unconstrained optimization problem. The fitness function $g(x)$ can be presented as in the following equation:

$$g(x) = f(x) + p(x) \tag{23}$$

where $p(x)$ is the penalty function and it is designed to be as follows:

$$p(x) = \sum_{i=1}^n \alpha_i \psi(h_{ci}(x)) \tag{24}$$

where ψ is Relu function, and α_i is the parameters that coordinate the value of the constraint function $h_c(x)$ when the constraint is violated.

The speed and position of the particles of PSO are operated by the following formula:

$$\begin{cases} v_q^{k+1} = w \times v_q^k + c_1 \times \zeta \times (x_{q(best)}^k - x_q^k) \\ \quad + c_2 \times \zeta \times (x_{g(best)}^k - x_q^k) \\ x_q^{k+1} = x_q^k + v_q^{k+1} \end{cases} \tag{25}$$

where v_q^k and x_q^k are the speed and position of the q th particle in the k th iteration, respectively, c_1 and c_2 are the learning factors, w is the inertia weight, $x_{q(pbest)}$ is the personal best of the q th particle, $x_{g(best)}$ is the global best of the swarm, and ζ is a random variable uniformly distributed in $(0, 1)$.

Inspired by Liu et al. [37], the parallel modified particle swarm optimization (PMPSO) algorithm is utilized to perform the constrained design optimization problem to minimize the cost of the offshore PCSH structure by operating the inertia weight and particle updating strategy. The inertia weight of the PMPSO can be estimated by the following formula:

$$\begin{cases} w(k) = r(k) \cdot w_{min} + (w_{max} - w_{min}) \cdot k / K \\ r(k+1) = 4r(k)(1 - r(k)) \\ r(0) = rand \end{cases} \tag{26}$$

where K is the maximum number of iterations, the minimum inertia weight w_{min} equals 0.4, and the maximum inertia weight w_{max} equals 0.9.

In each cycle, two distinct personal best particles are stochastically selected from the swarm, out of which the superior one is evaluated as a candidate personal best solution $x_{C(best)}^k$ to achieve the stochastic learning, which can enhance the ability of the algorithm to avoid premature. Then, the better one, by comparing $x_{q(best)}^k$ with $x_{C(best)}^k$ by their fitness value, will be adopted as the final stochastic personal best $x_{Sq(best)}^k$.

$$x_{C(best)}^k = argmin \{ g(x_{a(best)}^k), g(x_{b(best)}^k) \} \tag{27}$$

$$x_{Sq(best)}^k = \begin{cases} x_{C(best)}^k & g(x_{C(best)}^k) < g(x_{q(best)}^k) \\ x_{q(best)}^k & others \end{cases} \tag{28}$$

where $a \neq b \in \{1, 2, 3, \dots, Q\}$, Q is the number of particles.

The speed and position of the particles of PMPSO are continuously operated by the following formulas:

$$v_q^{k+1} = w(k)v_q^k + c_1\zeta_1 \otimes (x_{S(best)}^k - x_q^k) + c_2\zeta_2 \otimes (x_{M(best)}^k - x_q^k) \tag{29}$$

$$x_q^{k+1} = \begin{cases} w(k)x_q^k + (1 - w(k))v_q^{k+1} + x_{g(best)}^k & p_q > rand \\ x_q^k + v_q^{k+1} & others \end{cases} \quad (30)$$

$$p_q = \frac{\exp(g(x_q^k))}{\exp(\frac{1}{Q} \sum_{q=1}^Q g(x_q^k))} \quad (31)$$

$$x_{M(best)}^k = mean\{x_{1(best)}^k, x_{2(best)}^k, \dots, x_{Q(best)}^k\} \quad (32)$$

Shown in the following equations, the global worst particle $x_{g(worst)}^k$ will be substituted in every cycle to improve the diversity of the population.

$$x_{g(worst)}^k = argmax\{g(x_{1(best)}^k), g(x_{2(best)}^k), \dots, g(x_{Q(best)}^k)\} \quad (33)$$

$$x_{N(worst)}^k = x_{g(best)}^k + rand \cdot (x_{a(best)}^k - x_{b(best)}^k) \quad (34)$$

$$x_{g(worst)}^k = \begin{cases} x_{N(worst)}^k, & g(x_{N(worst)}^k) < g(x_{g(worst)}^k) \\ x_{g(worst)}^k, & others \end{cases} \quad (35)$$

4.3. Design Constraints for the Optimization

Referring to GB 50135-2006: Code for Design of High-Rising Structures [38], GB 50010-2010: Code for Design of Concrete Structures [39], GB 50011-2010: Code for Seismic Design of Buildings [35], GB50009-2012: Load Code for the Design of Building Structures [33], GB 50051-2013: Code for Design of Chimneys [40], GB 50017-2017: Code for Design of Steel Structure [41], JTS 167-2018: Design Code for Wharf Structures [42], ASCE/AWEA RP2011 [43], DNV-OS-J101 [44] and other relevant studies [45,46], in the optimization for the offshore PCSH support structures, a total of eleven design constraints, illustrated in Figure 5, are parallelly used to ensure the safety of the structure under both SLS and ULS by MATLAB R2016b to enhance the computing speed since the calculations between different particles are independent of each other [24].

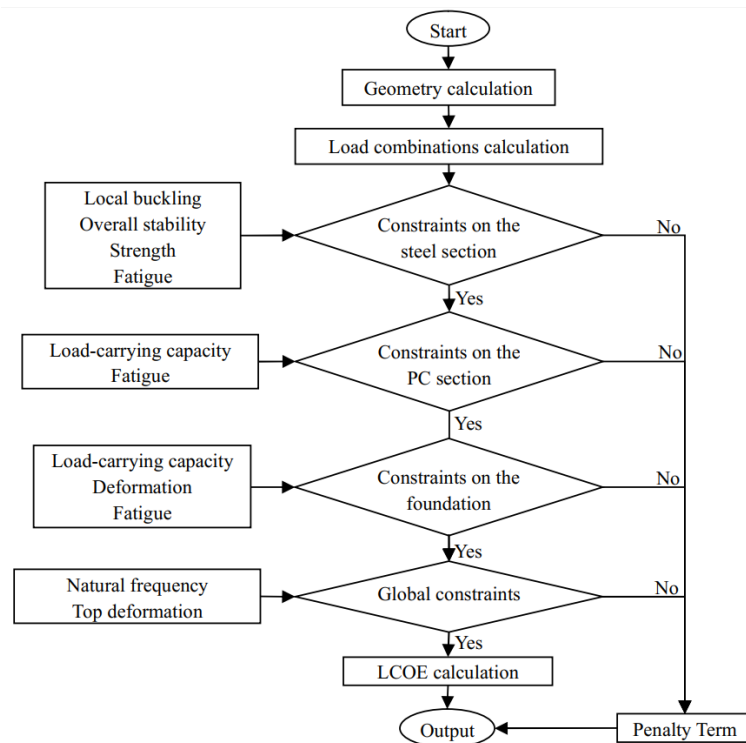


Figure 5. Flow chart of fitness evaluation for the offshore PCSH support with pile foundation.

The geometry constraints, including the minimum thickness of the steel and PC part, and the dimension requirements listed in Table 1, are restricted by generating the particles in a certain range. The outer diameter at the bottom of the substructure is constrained to ensure that that the structural dimensions are within the range where Morison’s equation applies.

5. Optimization Results

5.1. Design Parameters of the Offshore PCSH Support Structure

To testify the effectiveness of the optimization approach for the proposed PCSH wind turbine support with a pile foundation, a four-pile jacket-type 5.5 MW offshore wind turbine support structure with a hub elevation of 102.3 m is taken as an example. As an alternative of the example, a 5.5 MW offshore PCSH wind turbine support is designed and optimized based on the PMPSO algorithm. The parameters of the traditional four-pile jacket-type support structure and the wind farm are listed in Table 2. The cost of the original design is USD 2.72 million [47]. The material properties of concrete and steel determined by GB 50010-2010 are listed in Table 3 [39]. The elastic behavior of the soil is mainly considered, and its parameters are shown in Table 4. The optimal procedure is performed by MATLAB R2016b.

Table 2. Parameters of the wind turbine and wind farm.

Wind Turbine Parameter	Value
Rated power (kW)	5500
Designed wind zone class	IEC IB
Cut-in wind speed (m/s)	3
Rated wind speed (m/s)	10
Cut-out wind speed (m/s)	25
Extreme wind speed (m/s)	52.5
Designed lifetime (year)	25
Rotor diameter (m)	158
Swept area (m ²)	19,607
Wind turbine (t)	443
Rated rotational speed (rpm)	14
Capacity factor	0.5
Water depth (m)	25
Wavelength (m)	168.9
Wave height (m)	10.03
Wave period (s)	12.2

Table 3. Material properties of the offshore PCSH support.

Material	Elastic Modulus (MPa)	Density (kg/m ³)	Poisson’s Ratio	Compressive Strength (MPa)	Tensile Strength (MPa)
C60	36,000	2500	0.2	27.5	2.04
Q345	206,000	7850	0.28	295	-
HRB 400	200,000	7850	0.3	360	-
Strand	195,000	7850	0.3	1320	-
DH36	200,000	7850	0.3	355	-

Table 4. Material properties of the different soil layers used in analysis.

Type of Soil	Effective Unit Weight (kN/m ³)	Depth (m)	Subgrade Reaction (kN/m ³)	Angle of Friction (deg.)	Cohesion (kPa)	Lateral Frictional Resistance (kPa)	Uplift Coefficient
Cohesive soil	8.9	41.9	8800	28	2	30	0.65
Medium sand	9.9	64.2	33,600	38	2	85	0.54
Gravelly sand	10.8	92.3	40,400	38	2	120	0.77

5.2. Optimization Results and the Comparison of the Mathematical Behavior
 5.2.1. Algorithm Comparison

In this experimentation, the PSO algorithm is chosen to assess the performance of PMPSO. The PSO and PMPSO algorithms are independently run 30 times. Shown in Table 5, three indicators, average value (Avg), standard deviation (Std), and minimum (Min), are adopted to compare the performance of the PMPSO with that of the PSO. According to Table 5, the overall performance of the PMPSO is better than that of the PSO.

Table 5. Comparison of the optimal results between PSO and PMPSO.

	PSO	PMPSO
Avg	1.89	1.75
Std	0.0084	0.0032
Min	1.75	1.64

The relationships between the object function and the number of iterations of the PSO and PMPSO algorithms with the best optimal result are employed in Figure 6. The initial population of the particles in both the PSO and PMPSO are randomly generated at the beginning of the optimization. The cost of the PCSH support structure decreases sharply at the early phase of optimal procedure, and then gradually converges. The determined cost values with the PSO and PMPSO algorithms in the last optimization iterations are USD 1.75 and 1.64 million, respectively, which is lower than the original design of USD 2.72 million. It means that the cost of the optimized PCSH support structure with a pile foundation can be effectively reduced when compared with that of the traditional design. From Figure 6, it can be seen that the cost of the optimized PCSH support structure decreases fast even in the first iterations when PMPSO is employed. Moreover, the final optimal result with the PSO algorithm performs worse than that with the PMPSO algorithm, and the convergence performance of the PMPSO approach is superior to that of the PSO approach.

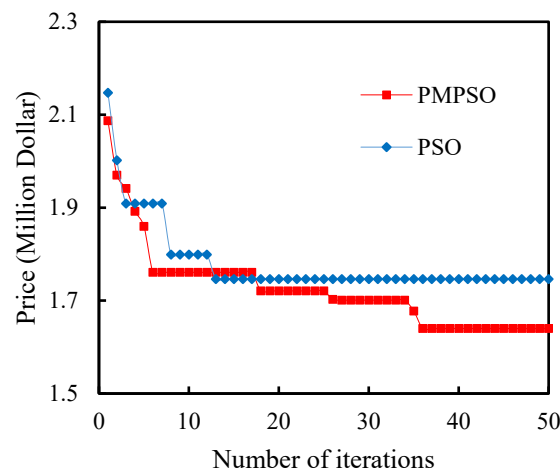


Figure 6. Convergence curve of PSO and PMPSO.

5.2.2. Optimization Result

The corresponding dimensions of the support structure optimized by the PSO and PMPSO algorithms are presented and compared in Table 6. According to Table 6, the steel section occupied about 21.5% and 25.8% of the overall height of the offshore support structure optimized by the PSO and PMPSO algorithms, respectively. Considering the maintenance cost and electricity generation, the levelized cost of energy, LCOE, a pivotal metric in the economic assessment of wind power generation system, is adopted to assess the comprehensive investment of the offshore PCSH support structure [48]. The LCOE of

the original design is 0.0771 USD/kWh. The LCOE of the results optimized by PSO and PMPSO are 0.0684 and 0.0680 USD/kWh, respectively. The proposed PCSH wind turbine support structure can reduce the comprehensive cost obviously.

Table 6. Optimized parts’ dimensions of the offshore PCSH support structure with PSO and PMPSO.

Variable	PSO	PMPSO
t_{st} (mm)	26	16
t_{sb} (mm)	33	22
H_s (mm)	27,500	33,000
D_{st} (mm)	4050	4050
D_{sb} (mm)	5934	6311
t_{ct} (mm)	200	220
t_{cb} (mm)	200	230
H_c (mm)	58,830	53,330
D_{ct} (mm)	5934	7340
D_{cb} (mm)	11,200	8500
t_{zt} (mm)	200	250
t_{zb} (mm)	200	300
H_z (mm)	41,500	41,500
D_{zt} (mm)	11,200	11,000
D_{zb} (mm)	35,350	35,350
x_b	27,133	20,000
y_b	8362	10,000
Prestressed reinforcement area (mm ²)	37,800	59,850
Pile length (m)	94	87
Pile diameter (mm)	2.4	2.4
LCOE (US dollar/kWh)	0.0684	0.0680

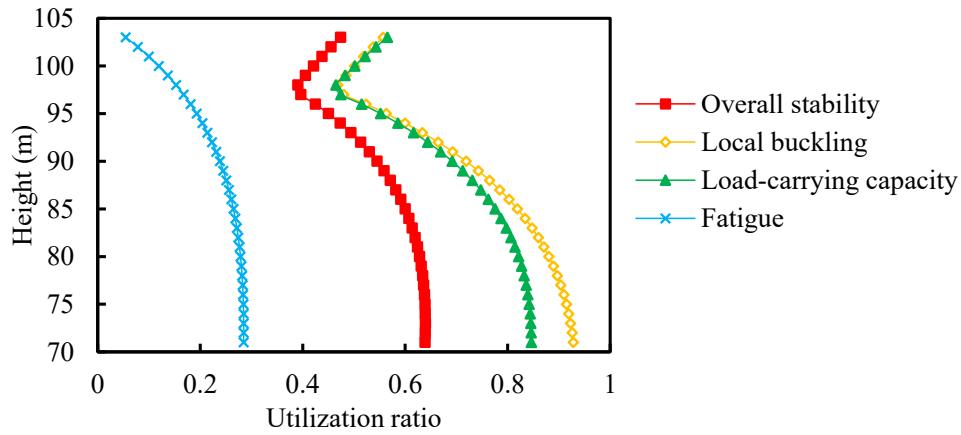
5.2.3. Materials’ Utilization Ratio

To investigate the efficiency of the offshore PCSH support tower optimized with the PMPSO algorithm, the materials’ utilization ratio of each part of the structure is analyzed, which is the ratio of the calculated value to the maximum permitted values under loading. The maximum material utilization ratios of the design of the offshore PCSH support structure optimized by the PSO and PMPSO algorithms are listed in Table 7. The utilization ratio for each constraint along the height of the structure optimized by the PMPSO is shown in Figure 7.

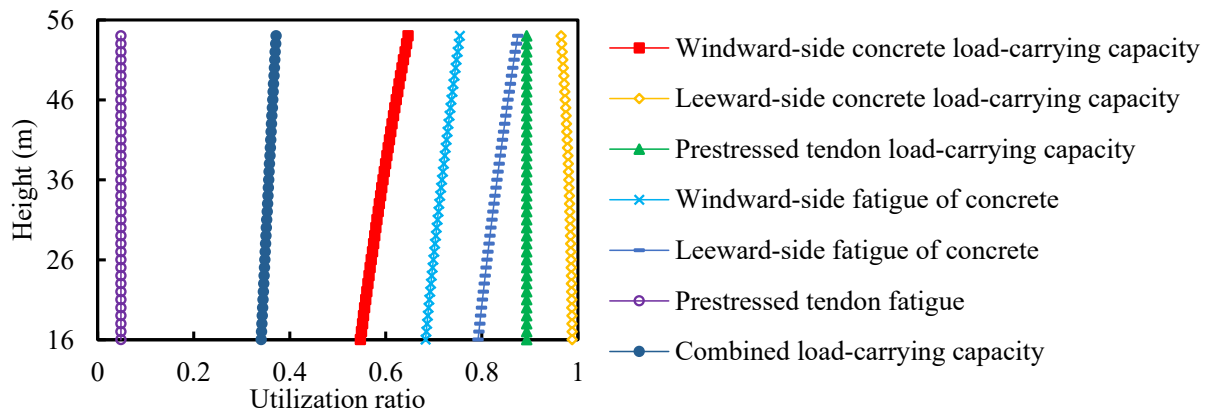
The material utilization ratio of the steel tube segment is shown in Figure 7a. It can be seen that a turning point at the elevation of about 96 m of the structure appears because the bending moment caused by the eccentricity of the RNA is opposite to that generated by wind loads. The material utilization ratio of the PC segment of the tower and the substructure for load-carrying capacity and fatigue is presented in Figure 7b,c, respectively. The utilization ratio of the load-carrying capacity of the leeward-side is close to one in Figure 7b, which means that the concrete was fully utilized. In Figure 7c, the utilization ratio of the substructure decreases rapidly at the lower part of the substructure, whose diameter increases greatly as shown in Figure 4c. A turning point at the height of about 10 m of the substructure can be seen in Figure 7c because the water load has a significant influence on the substructure. The material utilization ratios of the windward load-carrying capacity are larger than zero for both designs, which shows that the whole PC section, including the PC segment of the tower and the substructure, is under pressure.

From Table 7, the material utilization ratios of all constraints for the design optimized by the PSO and PMPSO are less than one but greater than zero. The PCSH support structure fulfills the relevant requirements. In the design optimized by PMPSO, the local buckling for the steel tube, the load-carrying capacity and the fatigue for the PC tube of the tower and the substructure are prominent because the three constraints have the largest maximum utilization ratio of all constraints in their respective segment. The maximum material utilization ratio of each segment is close to one, which validates the efficiency of

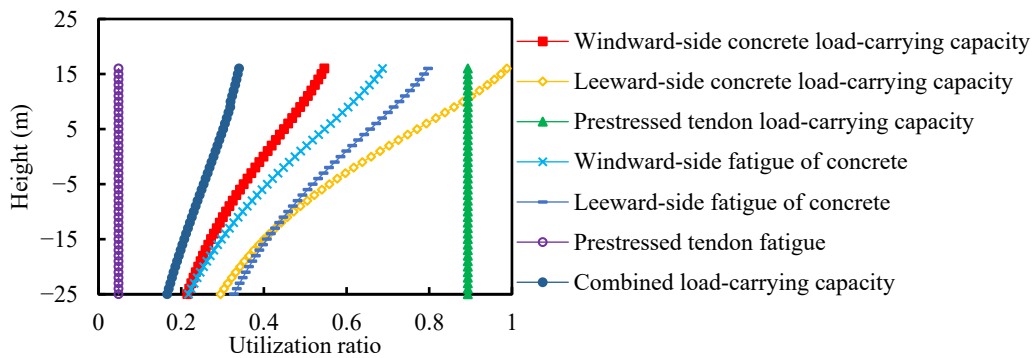
the PMPSO algorithm. However, in the design optimized by PSO, the maximum material utilization ratios are overall stability, the load-carrying capacity of prestressed tendon of PC, and the substructure segment. In addition, most of the utilization ratios of the design optimized by PSO are less than that of the design optimized by PMPSO. This is mainly caused by the premature convergence of the basic PSO algorithm.



(a) Steel segment



(b) PC segment



(c) Substructure

Figure 7. The utilization ratio of the offshore PCSH support structure optimized by the PMPSO.

Table 7. Maximum utilization ratio comparison of the PSO and PMPSO.

Design	Maximum Utilization Ratio	PSO	PMPSO
Steel segment	Overall stability	0.41	0.64
	Local buckling	0.37	0.93
	Load-carrying capacity	0.51	0.85
	Fatigue	0.18	0.28
PC segment	Windward-side concrete load-carrying capacity	0.47	0.62
	Leeward-side concrete load-carrying capacity	0.83	0.96
	Prestressed tendon load-carrying capacity	0.66	0.66
	Combined load-carrying capacity	0.09	0.08
	Windward-side fatigue of concrete	0.69	0.91
	Leeward-side fatigue of concrete	0.84	0.97
Substructure segment	Prestressed tendon fatigue	0.13	0.15
	Windward-side concrete load-carrying capacity	0.27	0.46
	Leeward-side concrete load-carrying capacity	0.57	0.91
	Prestressed tendon load-carrying capacity	0.65	0.67
	Combined load-carrying capacity	0.05	0.08
	Windward-side fatigue of concrete	0.33	0.68
	Leeward-side fatigue of concrete	0.57	0.92
Prestressed tendon fatigue	0.11	0.17	

5.2.4. Comparison of the First Natural Frequency of Different Support Structures

The rated rotational speed of the wind turbine is 14 rpm. The first natural frequency is required to be in the ‘soft-stiff’ range between 0.245 Hz (1P) and 0.48 Hz (3P). The first natural frequencies of the original tower and the PCSH towers optimized by PSO and PMPSO are 0.31 Hz, 0.45 Hz and 0.39 Hz, respectively. It can be seen that the first natural frequencies of the three different designs are within the allowable range. Compared with the original support structure, the PCSH support structures have higher natural frequencies and larger safety margins. Compared with the original support structure and the PCSH support structure optimized by PSO, the design optimized by the PMPSO algorithm has the largest safety margin to avoid the resonance due to the excitation of the wind turbine.

5.2.5. Comparison of the Maximum Top Deformation of Different Support Structures

The maximum deformations on the top of the original design and the optimized structure with PSO and PMPSO are provided in Table 8.

Table 8. Maximum deformation comparison of different supports.

Design	Top Displacement (mm)	Top Rotation (deg)
Original	953	1.09
PSO	408	0.50
PMPSO	622	0.74

From Table 8, it can be observed that the maximum displacement and rotation at the top of the supports for all of the three designs are less than $H/100$ and 5 deg, respectively. The displacements and rotations on the top of the offshore PCSH wind turbine support structures are smaller than those of the original design. The design optimized by the PSO algorithm has the smallest maximum displacement and rotation. The reason is that the lower PC part of the PCSH support structure optimized by the PSO is higher than that of the PCSH support structure optimized by the PMPSO, and a higher PC segment has higher stiffness.

5.2.6. Comparison of Weight of Different Support Structures

The comparison of the weights of the three wind turbine support structures is shown in Table 9. The consumption of steel of the design optimized by PSO and PMPSO is,

respectively, reduced by about 76.3% and 81.0%, which greatly reduced the cost of the structure. The weight of the optimized PCSH structure with a foundation is increased by about 51.8% and 40.7%, which strengthens the anti-overturning capacity of the PCSH wind turbine support structure.

Table 9. Weight comparison of different supports.

Design	Steel Section of the Tower (t)	Concrete Section of the Tower (t)	Substructure (t)	Foundation (t)	Total (t)
Original	426	-	815	711	1952
PSO	101	815	1296	751	2963
PMPSO	81	701	1240	724	2746

5.2.7. Comparison of Pile Foundation Parameters of Different Support Structures

The comparison of the parameters of the pile foundation of the different support structures is provided in Table 10. Compared with the four-pile jacket-type offshore wind turbine support structure, the maximum compressive load increased by about 16.20% and 3.44% for the design optimized by the PSO and PMPSO algorithm, respectively, and the maximum pullout load acting on the piles decreased by about 19.24% and 31.82%, respectively, because of the heavier weight of the PCSH support structures and larger wave load on the substructure.

Table 10. Pile foundation comparison.

Design	Original	PSO	PMPSO
Embedded depth (m)	75	79	76
Compressive carrying capacity (kN)	22,322	24,072	22,760
Pullout carrying capacity (kN)	22,175	23,926	22,613
Maximum compressive load under ULS (kN)	20,613	23,953	21,323
Maximum pullout load under ULS (kN)	13,555	10,947	9242
Maximum deflection (mm)	14.20	99.36	89.29
Maximum rotation (deg)	0.0406	0.1490	0.1318

The maximum deflections and rotations at the top of the piles are smaller than 0.1 m and 0.5 deg, respectively, indicating that the piles are structurally sound in terms of both displacement and rotation [44]. Compared with the original design, the maximum deflection and rotation at the top of the piles increased by 85.16 mm and 75.09 mm for the design optimized by the PMPSO algorithm and about 0.1084 deg and 0.0912 deg for the design optimized by the PSO algorithm. This is due to the alteration in the form of the structure, resulting in an increase in the wave forces on the structure. Therefore, the embedded length of the piles has been, respectively, extended by 4 m and 1 m to support the structure for the PSO and PMPSO optimized designs. However, considering that concrete structures are less expensive than steel structures, the total cost of the optimized structure is still lower than that of the original structure.

5.2.8. Comparison of Computational Efficiency for Optimization

The computing time for the optimization design of the offshore PCSH support structures with a pile foundation using PSO and PMPSO is 12,254 s and 4997 s, respectively. The computing time of the PMPSO can be reduced by 59.22% when compared with that of the PSO after reaching the maximum number of iterations.

6. Conclusions

This paper presented a PCSH support structure for offshore wind turbines that consists of a PCSH tower, a PC substructure, and a pile foundation, and a PMPSO algorithm was adopted to optimize the design of the proposed PCSH support tower with the pile

foundation used for the soft soil layer. The cost was considered as the optimization objective function under eleven optimization constraints. A 5.5 MW wind turbine supported by a steel tube and conventional jacket foundation was used as a reference model for comparison. The SSI and the effect of water pressure and earthquake were considered. The offshore PCSH wind turbine support structure with a pile foundation was modeled as a multi-degree-of-freedom system. A geometrically optimal result for the offshore PCSH support tower with the PMPSO algorithm was obtained and compared with that of the four-pile jacket-type offshore wind turbine support structure and the optimized results with PSO. Based on this study, the following conclusions can be made:

1. The cost of the optimized PCSH wind turbine support structure obviously decreases when compared with the original design, showing it is a cost-efficient alternative for traditional offshore wind support structures for lower cost requirements.
2. The height of the steel tube is recommended to occupy about 25.8% of the overall height of the PCSH support structure for offshore wind turbine.
3. Compared with the four-pile jacket-type offshore wind turbine support structure, the optimized offshore PCSH support structure can provide better mechanic behavior, including the first natural frequency, top deformation, and anti-overturning capacity.
4. The PMPSO algorithm provides better performance compared to the PSO algorithm. Fulfilling the design constraints, the PMPSO algorithm provides a more affordable primary optimal design for the PCSH support structures for offshore wind turbines with a pile foundation with considerably improved computational efficiency.

In this study, the PCSH support structure is assumed as a linear structure with small deformation. Further studies are desired for the optimization of the PCSH support structure with numerical and experimental analysis when the material's nonlinearity, geometric nonlinearity, construction time and adaptability to site-specific conditions are considered.

Author Contributions: Conceptualization, B.X. and G.Y.; methodology, B.X.; software, B.X.; validation, B.X. and Z.L.; formal analysis, B.X.; investigation, Z.L.; resources, G.Y.; data curation, Z.L.; writing—original draft preparation, Z.L.; writing—review and editing, B.X.; visualization, Z.L.; supervision, B.X.; project administration, B.X.; funding acquisition, B.X. All authors have read and agreed to the published version of the manuscript.

Funding: This research was funded by the National Natural Science Foundation of China (51878305; 51478175) and the Scientific Research Funds of Huaqiao University (605-50Y18016).

Institutional Review Board Statement: Not applicable.

Informed Consent Statement: Not applicable.

Data Availability Statement: The data that support the findings of this paper are available upon request.

Conflicts of Interest: Author Guokai Yuan was employed by the company China Energy Engineering Group Guangdong Electric Power Design Institute Co., Ltd. The remaining authors declare that the research was conducted in the absence of any commercial or financial relationships that could be construed as a potential conflict of interest.

References

1. Mendes, P.; Correia, J.A.F.O.; Mourão, A.; Pereira, R.; Fantuzzi, N.; De Jesus, A.; Calçada, R. Fatigue Assessments of a Jacket-Type Offshore Structure Based on Static and Dynamic Analyses. *Pract. Period. Struct. Des. Constr.* **2021**, *26*, 04020054. [[CrossRef](#)]
2. Arvan, P.A.; Raju, R.D.; Arockiasamy, M. Offshore Wind Turbine Monopile Foundation Systems in Multilayered Soil Strata under Aerodynamic and Hydrodynamic Loads: State-of-the-Art Review. *Pract. Period. Struct. Des. Constr.* **2023**, *28*, 03123001. [[CrossRef](#)]
3. Wang, Y.-G. Predicting Loads and Dynamic Responses of An Offshore Jacket Wind Turbine in A Nonlinear Sea. *China Ocean Eng.* **2020**, *34*, 641–650. [[CrossRef](#)]
4. Campione, G. Simplified calculation model for offshore wind tower founded on monopile member. *Structures* **2023**, *51*, 962–969. [[CrossRef](#)]
5. Aidibi, A.; Babamohammadi, S.; Fatnuzzi, N.; Correia, J.A.F.O.; Manuel, L. Stress Concentration Factor Evaluation of Offshore Tubular KT Joints Based on Analytical and Numerical Solutions: Comparative Study. *Pract. Period. Struct. Des. Constr.* **2021**, *26*, 04021047. [[CrossRef](#)]

6. Kim, B.J.; Plodpradit, P.; Kim, K.D.; Kim, H.G. Three-dimensional Analysis of Prestressed Concrete Offshore Wind Turbine Structure Under Environmental and 5-MW Turbine Loads. *J. Mar. Sci. Appl.* **2018**, *17*, 625–637. [[CrossRef](#)]
7. Tu, W.; He, Y.; Liu, L.; Liu, Z.; Zhang, X.; Ke, W. Time Domain Nonlinear Dynamic Response Analysis of Offshore Wind Turbines on Gravity Base Foundation under Wind and Wave Loads. *J. Mar. Sci. Eng.* **2022**, *10*, 1628. [[CrossRef](#)]
8. Vølund, P. Concrete is the Future for Offshore Foundations. *Wind Eng.* **2005**, *29*, 531–563. [[CrossRef](#)]
9. Ma, H.; Yang, J. A novel hybrid monopile foundation for offshore wind turbines. *Ocean Eng.* **2020**, *198*, 106963. [[CrossRef](#)]
10. Lian, J.; Ding, H.; Zhang, P.; Yu, R. Design of large-scale prestressing bucket foundation for offshore wind turbines. *Trans. Tianjin Univ.* **2012**, *18*, 79–84. [[CrossRef](#)]
11. Zhai, H.; Ding, H.; Zhang, P.; Le, C. Model Tests of Soil Reinforcement Inside the Bucket Foundation with Vacuum Electroosmosis Method. *Appl. Sci.* **2019**, *9*, 3778. [[CrossRef](#)]
12. Chen, J.; Li, J.; Wang, D.; Feng, Y. Seismic response analysis of steel–concrete hybrid wind turbine tower. *J. Vib. Control* **2021**, *28*, 2240–2253. [[CrossRef](#)]
13. Huang, X.; Li, B.; Zhou, X.; Wang, Y.; Zhu, R. Geometric optimisation analysis of Steel–Concrete hybrid wind turbine towers. *Structures* **2022**, *35*, 1125–1137. [[CrossRef](#)]
14. Li, Z.; Xu, B.; Wang, J.; Chen, H.; Ge, H. Experimental and two-scale numerical studies on the behavior of prestressed concrete-steel hybrid wind turbine tower models. *Eng. Struct.* **2023**, *279*, 115622. [[CrossRef](#)]
15. Kim, H.G.; Kim, B.J. Feasibility study of new hybrid piled concrete foundation for offshore wind turbine. *Appl. Ocean Res.* **2018**, *76*, 11–21. [[CrossRef](#)]
16. O’Leary, K.; Pakrashi, V.; Kelliher, D. Optimization of composite material tower for offshore wind turbine structures. *Renew. Energy* **2019**, *140*, 928–942. [[CrossRef](#)]
17. Yeter, B.; Garbatov, Y.; Guedes Soares, C. Risk-based life-cycle assessment of offshore wind turbine support structures accounting for economic constraints. *Struct. Saf.* **2019**, *81*, 101867. [[CrossRef](#)]
18. Kaveh, A.; Sabeti, S. Structural optimization of jacket supporting structures for offshore wind turbines using colliding bodies optimization algorithm. *Struct. Des. Tall Spec. Build.* **2018**, *27*, e1494. [[CrossRef](#)]
19. Natarajan, A.; Stolpe, M.; Njomo Wandji, W. Structural optimization based design of jacket type sub-structures for 10 MW offshore wind turbines. *Ocean Eng.* **2019**, *172*, 629–640. [[CrossRef](#)]
20. Mathern, A.; Penadés-Plà, V.; Armesto Barros, J.; Yepes, V. Practical metamodel-assisted multi-objective design optimization for improved sustainability and buildability of wind turbine foundations. *Struct. Multidiscip. Optim.* **2022**, *65*, 46. [[CrossRef](#)]
21. Zhang, P.; Ding, H.; Le, C. Hydrodynamic motion of a large prestressed concrete bucket foundation for offshore wind turbines. *J. Renew. Sustain. Energy* **2013**, *5*, 063126. [[CrossRef](#)]
22. Kim, H.-G.; Kim, B.-J.; Lee, K.-H. Analysis of Piled Concrete Foundation for a 3-MW Class Offshore Wind Turbine along the Southwest Coast in Korea. *J. Mar. Sci. Eng.* **2020**, *8*, 215. [[CrossRef](#)]
23. Chen, J.; Li, J.; He, X. Design optimization of steel–concrete hybrid wind turbine tower based on improved genetic algorithm. *Struct. Des. Tall Spec. Build.* **2020**, *29*, e1741. [[CrossRef](#)]
24. Li, Z.; Chen, H.; Xu, B.; Ge, H. Hybrid Wind Turbine Towers Optimization with a Parallel Updated Particle Swarm Algorithm. *Appl. Sci.* **2021**, *11*, 8683. [[CrossRef](#)]
25. Yang, W.; Li, Q. A new added mass method for fluid-structure interaction analysis of deep-water bridge. *KSCE J. Civ. Eng.* **2013**, *17*, 1413–1424. [[CrossRef](#)]
26. Lu, S.; Lin, Y. *Calculation and Analysis of Pile Foundation*; China Communications Press: Beijing, China, 1987.
27. Liu, J.L. *Design and Calculation of Pile Foundation*; China Architecture & Building Press: Beijing, China, 1990.
28. Niu, W. Natural Frequency of Mono-pile Wind Turbine Considering Interaction between Pile and Elastic Foundation. *China Earthq. Eng. J.* **2016**, *38*, 713–719.
29. Dagli, B.Y.; Tuskan, Y.; Gökkuş, Ü. Evaluation of Offshore Wind Turbine Tower Dynamics with Numerical Analysis. *Adv. Civ. Eng.* **2018**, *2018*, 3054851. [[CrossRef](#)]
30. USACE. *Shore Protection Manual*; Department of the Army, Waterways Experiment Station, Corps of Engineers, Coastal Engineering Research Center: Vicksburg, MS, USA, 1984.
31. Maâtoug, M.A.; Ayadi, M. Numerical simulation of the second-order Stokes theory using finite difference method. *Alex. Eng. J.* **2016**, *55*, 3005–3013. [[CrossRef](#)]
32. Klaver, E.C. Static loads and dynamic loads of wind turbine tower. *Wind Power* **1989**, *3*, 44–49.
33. GB50009-2012; Load Code for the Design of Building Structures. Standardization Administration of China: Beijing, China, 2012.
34. AlHamaydeh, M.; Barakat, S.; Nasif, O. Optimization of Support Structures for Offshore Wind Turbines Using Genetic Algorithm with Domain-Trimming. *Math. Probl. Eng.* **2017**, *2017*, 5978375. [[CrossRef](#)]
35. GB 50011-2010; Code for seismic design of buildings. Standardization Administration of China: Beijing, China, 2010.
36. DNVGL-ST-0437; Loads and Site Conditions for Wind Turbines. Det Norske Veritas: Oslo, Norway, 2016.
37. Liu, H.; Zhang, X.-W.; Tu, L.-P. A modified particle swarm optimization using adaptive strategy. *Expert Syst. Appl.* **2020**, *152*, 113353. [[CrossRef](#)]
38. GB 50135-2006; Code for Design of High-Rising Structures. Standardization Administration of China: Beijing, China, 2007.
39. GB 50010-2010; Code for Design of Concrete Structures. Standardization Administration of China: Beijing, China, 2010.
40. GB 50051-2013; Code for Design of chimneys. Standardization Administration of China: Beijing, China, 2013.

41. GB 50017-2017; Code for Design of Steel Structure. Standardization Administration of China: Beijing, China, 2017.
42. JTS 167-2018; Design Code for Wharf Structures. MOT: Beijing, China, 2018.
43. Agbayani, N.A. Agbayani, N.A. A Technical Overview of ASCE/AWEA RP2011: Recommended Practice for Compliance of Large Land-Based Wind Turbine Support Structures. In *Structures Congress 2014*; ASCE Library: Reston, VA, USA, 2014; pp. 1759–1770.
44. DNV. *Design of Offshore Wind Turbine Structures*; Det Norske Veritas: Oslo, Norway, 2013.
45. Huo, T.; Tong, L. An approach to wind-induced fatigue analysis of wind turbine tubular towers. *J. Constr. Steel Res.* **2020**, *166*, 105917. [[CrossRef](#)]
46. Grünberg, J.; Joachim, G. *Concrete Structures for Wind Turbines*; John Wiley & Sons: Hoboken, NJ, USA, 2013.
47. Zheng, R.; Zhuang, J. *Special Report on Wind Turbine Foundation and Booster Station Foundation*; Energy Engineering Group Guangdong Electric Power Design Institute Co., Ltd.: Guangzhou, China, 2020.
48. Zakir, M.N.; Abasin, A.R.; Irshad, A.S.; Elias, S.; Yona, A.; Senjyu, T. Practical Wind Turbine Selection: A Multicriterion Decision Analysis for Sustainable Energy Infrastructure. *Pract. Period. Struct. Des. Constr.* **2024**, *29*, 04024028. [[CrossRef](#)]

Disclaimer/Publisher’s Note: The statements, opinions and data contained in all publications are solely those of the individual author(s) and contributor(s) and not of MDPI and/or the editor(s). MDPI and/or the editor(s) disclaim responsibility for any injury to people or property resulting from any ideas, methods, instructions or products referred to in the content.